

A simplified analysis of the behavior of suspension bridges under live load

Leonidas T. Stavridis[†]

Structural Engineering, National Technical University of Athens, Vas. Sofias 100-11528, Athens, Greece

(Received May 16, 2007, Accepted October 6, 2008)

Abstract. Having established the initial geometry and cable force of a typical three span suspension bridge under permanent load, the additional maximum response of the cable and the stiffening girder due to live load are determined, by means of an analytic procedure, considering the girder first hinged at its ends and then continuous through the main towers. The problem of interaction between the cable and the stiffening girder is examined taking under due consideration the second order effects, whereby, through the analogy to a fictitious tensioned beam under transverse load, a closed –form solution is achieved by means of a simple quadratic equation. It is found that the behavior of the whole system is governed by five simple dimensionless parameters which enable a quick determination of all the relevant design magnitudes of the bridge. Moreover, by introducing these parameters, a set of diagrams is presented, which enable the estimation of the influence of the geometric and loading data on the response and permit its immediate evaluation for preliminary design purposes.

Keywords: suspension bridge; stiffening girder; static analysis; design.

1. Introduction

The suspension bridge is the structural system which is adequate for crossing very long spans and as such it has been established over many years in the engineering history of mankind, achieving nowadays a high level of performance in all the technologically advanced countries (Ryall *et al.* 2000, Wai-Fah *et al.* 1999).

In the typical configuration of a three span suspension bridge with a deck supported by earth anchored cables, a primary characteristic representing always an essential design decision, is the continuity or not of the stiffening girder over the supports of the main towers. Although the majority of the constructed suspension bridges follows the scheme of the hinged connection of the girder with the towers, the continuous girder may be sometimes adopted, for example when a better runnability has to be ensured, or in order to overcome the maintenance problems arising from the expansion joints.

Such a structural system - either with hinged girders or not - consisting of a main and two side spans, has been tackled analytically in the past, through the so called deflection theory which has

[†] Associate Professor, Ph.D., E-mail: stavrel@central.ntua.gr

been developed many years ago, taking in consideration the deformability of the cable and the following identical deflection of the girder. The procedure involved in order to take into account these second order effects leads, according to the classical publications on the subject (Steinman 1935) and (Timoshenko 1943), to cumbersome and laborious calculations which do not permit an overview of the influence of various factors on the structural performance of the system.

Clearly, the subsequent development of the finite element method and the use of computer programs with nonlinear analysis capabilities, has overrun the above method. An analogous procedure in this numerical direction has been published as early as in (Brotton 1963), whereas the application of these methods to the analysis of suspension bridges is shown in (Jennings and Mairs 1972) and (Arzoumanidis and Bienek 1985) .

As these discretization methods cannot show on a quantitative basis the relative influence of the design parameters (main and side span lengths, cable profile, cable section area, girder moment of inertia, dead and live load) on the response, there is an obvious need for more direct and simple methodology helping to understand the behavior of the structure and providing a tool to perform quickly an analytically correct preliminary design. Of course, there are also design criteria regarding e.g. aerodynamic actions which have to be additionally taken into account, but, even if a sensitivity analysis of structural dynamic parameters is useful for the design (Liu *et al.* 1999), the problem of static response remains of essential importance.

An interest towards this direction has been already expressed through the works of (Cobo *et al.* 2001), (Clemente *et al.* 2000) and (Wollmann 2000), but none of these publications enable a direct analytic control of the suspension bridge behavior, on the basis of the above mentioned initially selected design parameters, especially in the case of a continuous stiffening girder.

The present paper is also oriented towards the same issue, aiming to provide a simple tool for the analysis of a suspension bridge on a purely analytical base, by considering firstly a two-hinge stiffening girder and secondly a continuous one, in order to determine the response of the cable and the girder under the action of the live load.

After reviewing the derivation of the fundamental equation of the deflection theory by considering the influence of the deformed geometry under an applied live load , the problem is reduced to that one of a fictitious tensioned beam transversely loaded, permitting in this way the determination of the unknown additional cable force through a simple quadratic algebraic equation which, although “approximative”, provides nevertheless an absolutely satisfactory accuracy.

Using this result also for the case of a continuous stiffening girder, the problem reduces to that one of restoring the compatibility of deformation of three fictitious tensioned beams subjected to a transverse load and applied end moments,

It is shown that the behavior of the whole system is governed by five dimensionless design parameters, namely :1) the sag to span ratio of the cable, 2) the initial strain of the cable under the dead load, 3) the ratio of live to dead load , 4) the ratio of the deflection of the simple girder under the dead load to the cable sag and - for the case of continuous girder - 5) the ratio of the side to main span.

The determination of the maximum static response of the system under the most unfavorable location of the live load for each specific case, is made possible using only these five dimensionless parameters, through a direct procedure easily programmable in a personal computer. This procedure enables also a parametric study resulting in dimensionless diagrams which show the influence of these parameters on the maximum cable force, the maximum span and support bending moments, as well as the maximum deflection of the stiffening girder.

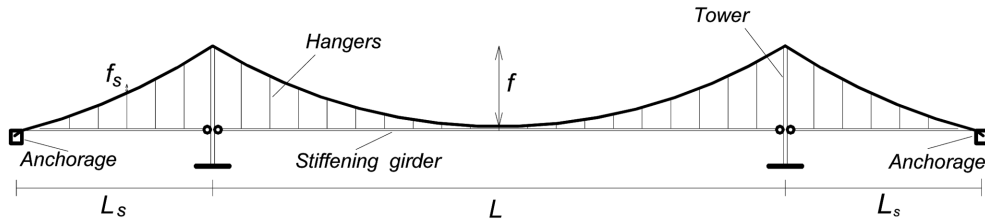


Fig. 1 Structural layout

2. Analysis

The earth anchored structural system is depicted in Fig. 1, with one main span of length L and two equal side spans of length L_s . It is assumed, following the usual practice, that the height of the tower over the deck practically equals the main cable sag and moreover, that the cable overrides the top of the towers without friction. The last assumption permits one to ignore in this context the influence of the deformation of the towers on the system's response.

Now, the horizontal component H_g of the cable tensile force is appropriately calibrated with respect to the desired sag f , so that for the existing dead load g (cable self weight included), the deck takes an absolutely horizontal position. The same conditions also hold for the side spans of length L_s and cable sag f_s . According to the previous assumption it will be

$$H_g = g \cdot L^2 / (8 \cdot f) = g \cdot L_s^2 / (8 \cdot f_s) \quad (1)$$

and consequently, as the two cable parts exhibit the same curvature, it must hold

$$f_s = L \cdot \beta^2 \cdot \lambda \quad (2)$$

where

$$\beta = L_s / L \text{ and } \lambda = f / L \quad (3)$$

In this way the bending of the girder is kept to a negligible level, given the small distance of the hangers. Nevertheless the action of an additional live load p on the girder tends to deform the cable and this additional cable deflection η will be imposed exactly the same on the stiffening girder, due to the assumed inextensibility of the hangers. The resulting increase in cable force will be represented by its horizontal component H_p . The purpose of the analysis consists in determining both these quantities.

The girder should be able to restrict the cable deflection due to the live load and at the same time to resist the bending resulting from this same deflection, as mentioned above.

The girder is subjected to a total load $q(x)$, consisting of the permanent load g , a live load p acting on a specified length and the actions $q_c(x)$ of the hangers directed upwards which, due to the small distances of the hangers, can be considered as continuously distributed (Fig. 2). It is

$$q(x) = -q_c(x) + g + p \quad (4)$$

The loadings g and p can be considered uniform but the loading $q_c(x)$ changes along the girder length. As this loading is applied also to the cable, the latter assumes a new funicular shape different from the initial parabolic one due to the uniform load g .

According to Fig. 3, the new cable geometry is described by $z(x)$, equal to

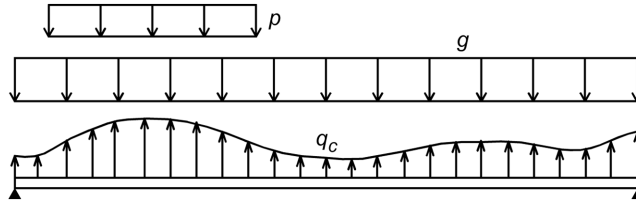


Fig. 2 Acting forces on the girder

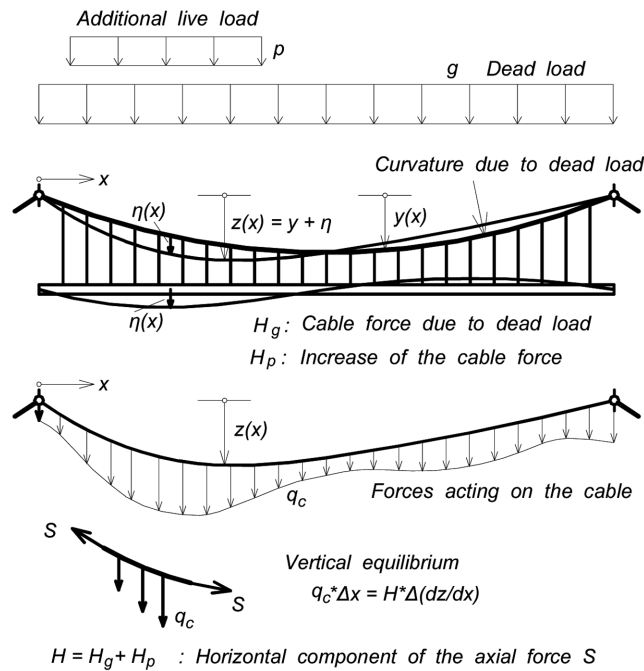


Fig. 3 Cable deformation under direct action of live load

$$z(x) = y(x) + \eta(x) \tag{5}$$

and the vertical equilibrium of an elementary cable segment yields

$$q_c(x) = \frac{d^2 z}{dx^2} (H_g + H_p) \tag{6}$$

with $(H_g + H_p)$ representing the horizontal component of its total axial force.

As the girder deflection $\eta(x)$ has to obey to the classical beam equation

$$EI \frac{d^4 \eta}{dx^4} = q(x) \tag{7}$$

on the basis of Eqs. (4) and (6) and given that $(d^2 y/dx^2)$ represents the negative cable curvature R under the load g , it may be obtained

$$EI \frac{d^4 \eta}{dx^4} - \frac{d^2 \eta}{dx^2} (H_g + H_p) = p - \frac{H_p}{R} \tag{8}$$

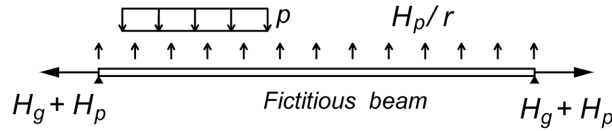


Fig. 4 Acting forces on the fictitious beam

This equation which is the basic differential equation of the “deflection theory of suspension bridges” (Timoshenko 1943, O’Connor 1971), may be recognized as the equation of a fictitious simple beam, having a transverse load $(p - H_p/R)$ and subjected to an axial tensile load $(H_g + H_p)$, according to the second order theory of beams (Fig. 4). This equation applies for a two-hinged stiffening girder, but nevertheless is also valid for a continuous girder, simulated by a fictitious continuous beam under the same transverse and axial load as above, taking into account the effects of the second order theory.

The deflection $\eta(x)$ of a simple beam due to a transverse load q and subjected to a tensile force H , is obtained from the following expression (Timoshenko 1956)

$$\eta(x) = \frac{q}{H} \left[\frac{\cosh(k \cdot L/2 - k \cdot x)}{k^2 \cdot \cosh(k \cdot L/2)} - \frac{1}{k^2} + \frac{x \cdot (L-x)}{2} \right] \tag{9}$$

whereas due to a concentrated moment M at the left or at the right support (Fig. 5), it is respectively

$$\eta(x) = \frac{M}{H} \left[\frac{L-x}{L} - \frac{\sinh(k \cdot L - k \cdot x)}{\sinh(k \cdot L)} \right] \quad \text{or} \quad \eta(x) = \frac{M}{H} \left[\frac{x}{L} - \frac{\sinh(k \cdot x)}{\sinh(k \cdot L)} \right] \tag{10}$$

with

$$k = \sqrt{\frac{H}{EI}} \tag{11}$$

2.1 Single span (hinged) stiffening girder

For the case of a two-hinged stiffening girder, the deflection function $\eta(x)$ in Eq. (9) can be

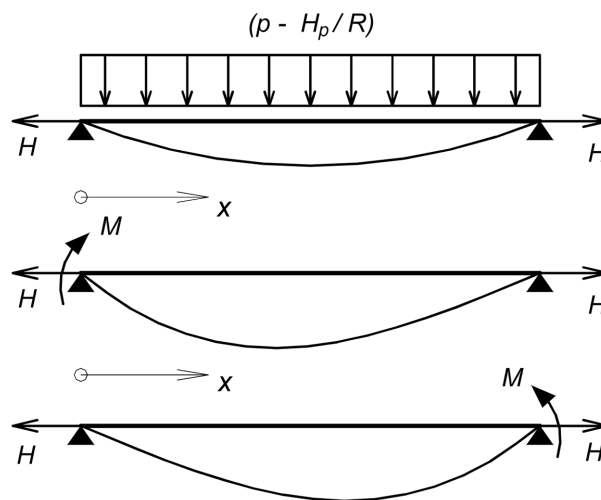


Fig. 5 Tensioned beam under transverse and end-moment loading

approximated quite satisfactorily for practical purposes, according to an established result of the second order theory of beams (Roik 1983), from the relation

$$\eta = W_1 \cdot \frac{1}{1 + \frac{H_g + H_p}{P_{cr}}} \quad (12)$$

where W_1 represents the (first order) deflection line of the simply supported beam under the load $(p - H_p/R)$ and P_{cr} its buckling load, equal to $(\pi^2 EI/L^2)$.

Now, the increase H_p of the cable force H_g of a cable fixed at its ends is related to its additional deflection η through the relation (Timoshenko 1943)

$$\frac{H_p}{A_c E_c} * L_c = \frac{g}{H} \int_0^L \eta dx - \frac{1}{2} \int_0^L \frac{d^2 \eta}{dx^2} * \eta * dx \quad (13)$$

where, for ratios λ between 1/8 and 1/12, i.e., the prevailing range for suspension bridges, the length L_c is given with good approximation from the expression

$$L_c = L * \left[\frac{1}{\cos^3 \alpha} + 8 * \lambda^2 \frac{1}{\cos \alpha} \right] \quad (14)$$

with α representing the inclination angle of the line connecting the two cable ends, which for the examined case equals zero.

The omission of the second integral term in the right side of Eq. (13) affects for long spans very little the overall accuracy, so it can be written more simply

$$\frac{H_p}{A_c E_c} * L_c = \frac{g}{H_{g_0}} \int_0^L \eta dx \quad (15)$$

It is understood that the unknown magnitude H_p can be determined from the condition that the deflection curve $\eta(x)$ according to Eq. (12) - or (more strictly) according to Eq. (9) - must also satisfy the "cable equation" (15).

Now, in the usual design practice, two loading configurations for the live load p have to be taken into account, namely one acting on the left half of the girder span and the second one extending over the whole span. The first loading yields the maximum deflection and subsequently the most unfavorable girder bending, whereas the second one yields the maximum value of cable force.

In the first case the load p is equivalent to the action of a symmetrical load $(p/2)$ over the whole span and an antisymmetric one $(p/2)$, as shown in Fig. 6. The deflection line $\eta(x)$ of the fictitious beam can be equally evaluated from the superposition of the deflection η_{sym} due to symmetric loading $(p/2 - H_p/R)$ over the whole span and of the deflection η_{ant} due to the antisymmetric loading $(p/2)$ according to Fig. 6. It is noted that this superposition is possible, given the constant axial load of the beam. After these considerations and given that

$$\int_0^L \eta_{ant} dx = 0 \quad (16)$$

the last Eq. (15) is written

$$\frac{H_p}{A_c E_c} * L_c = \frac{g}{H_{g_0}} \int_0^L \eta_{sym} dx \quad (17)$$

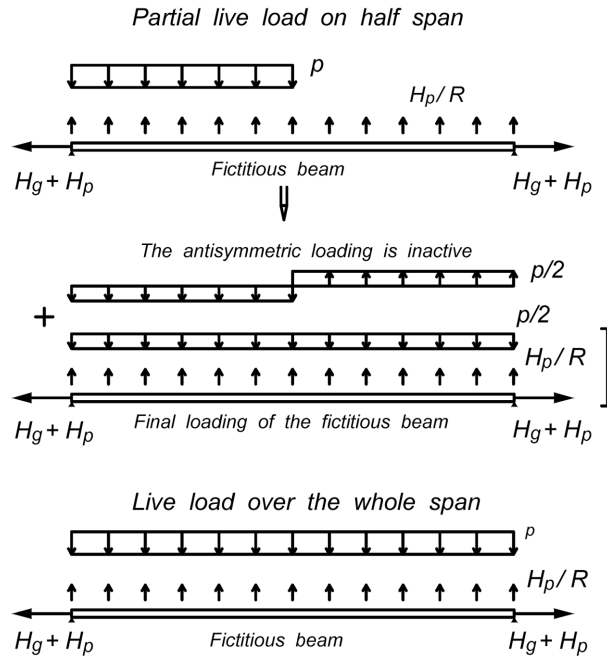


Fig. 6 Characteristic positions of live load on the fictitious beam

It is obvious that this relation is valid also for the second case where the fictitious beam is loaded with $(p - H_p/R)$ over its whole length.

According to the previous examination, η_{sym} can be determined with satisfactory accuracy from the expression

$$\eta_{sym} = W_1 \cdot \frac{1}{1 + \frac{H_g + H_p}{P_{cr}}} \tag{18}$$

where W_1 represents the deflection line of the simple beam under the transverse load

$(p^* - H_p/R)$ with p^* equal either to $p/2$ for the partial loading of the left half of the span, or to p for the loading of the whole span.

The deflection line W_1 of the beam results according to the well known Mohr's theorem, as the bending diagram of the simply supported beam under the load (M_1^0/EI) , where M_1^0 is the function of the bending moment of the beam due to the loading $(p^* - H_p/R)$.

It is obtained

$$W_1(x) = \frac{(p^* - H_p/R) * L^4}{24 * EI} \left[\left(\frac{x}{L}\right)^4 - 2 * \left(\frac{x}{L}\right)^3 + \left(\frac{x}{L}\right) \right] \tag{19}$$

Substituting Eqs. (18) and (19) into Eq. (17), leads to the following algebraic equation for the unknown H_p

$$\frac{H_p}{A_c E_c} * L_c = \frac{g}{H_g} \left[\frac{(p^* - H_p/R) * L^5}{120 * EI} \frac{1}{1 + \frac{H_g + H_p}{P_{cr}}} \right] \tag{20}$$

At this stage the following dimensionless parameters may be introduced

$$G = \frac{H_g \cdot L^2}{E \cdot I}, \quad \gamma = \frac{p^*}{g}, \quad \varepsilon = \frac{H_g}{A_c \cdot E_c} \quad (21)$$

as well as the unknown parameter of the problem

$$Z = \frac{H_p}{H_g} \quad (22)$$

It is noted that the parameter G represents the ratio of the deflection of the simply supported girder under the dead load to the cable sag, multiplied by the factor $(48/5)$, whereas the parameter ε represents the strain of the cable at its lowest point due to the dead load g .

The last Eq. (20) can now be written

$$Z^2 + \left(\frac{\pi^2}{G} + \omega + 1\right) \cdot Z - \gamma \cdot \omega = 0 \quad (23)$$

where

$$\omega = \frac{8 \cdot \pi^2}{15 \cdot \varepsilon} \cdot \frac{1}{1/\lambda^2 + 8} \quad (24)$$

so that Z may be readily determined from the above quadratic equation according to the expression

$$Z = -\zeta + \sqrt{\zeta^2 + \rho} \quad (25)$$

with

$$\zeta = \left(\frac{1}{2}\right) \cdot \left(\frac{\pi^2}{G} + \omega + 1\right) \quad \text{and} \quad \rho = \gamma \cdot \omega \quad (26)$$

On the other side, substituting into Eq. (17) the exact expression of $\eta(x)$ from Eq. (9), performing the indicated integrations and considering the above introduced parameters, the following equation is obtained

$$Z \cdot \varepsilon \cdot (1 + 8 \cdot \lambda^2) = 64 \cdot \lambda^2 \cdot \frac{\gamma - Z}{Z + 1} \cdot \left[\frac{2 \cdot \sinh(D/2)}{D^3 \cdot \cosh(D/2)} - \frac{1}{D^2} + \frac{1}{12} \right] \quad (27)$$

with

$$D = \sqrt{G \cdot (Z + 1)} \quad (28)$$

It is found that the value of Z obtained from Eq. (25) differs from the exact solution of the above not directly solvable Eq. (27) by less than 1%, a fact which allows to consider the former value as the proper solution of the problem.

2.2 Continuous stiffening girder

The fictitious continuous beam according to Eq. (8), may now be considered as a system of three simply supported beams having the same axial load, a respective transverse load and additional end moments appropriately applied, in order to guarantee the continuity at the supports (Fig. 7).

Referring now to the fictitious continuous beam loaded symmetrically as shown in Fig. 7, the support moment M is determined from the requirement that the end slopes φ_L and φ_R of the constituent simple beams have to be at each support equal. These slopes are obtained for the left support on the basis of Eqs. (9) and (10).

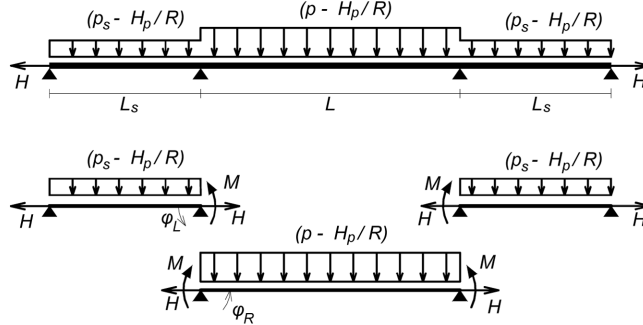


Fig. 7 Continuous girder under transverse and axial load

Using the above introduced dimensionless parameters according to the Eqs. (3), (21), (22) and (28), the support moment M is determined according to the following expression

$$M = g \cdot L^2 \cdot m_{sym} \tag{29}$$

where

$$m_{sym} = \frac{1}{D^2} \frac{(\gamma_S - Z) \cdot [(\beta \cdot D/2) - \tanh(\beta \cdot D/2)] + (\gamma - Z) \cdot [D/2 - \tanh(D/2)]}{\frac{1}{\beta \cdot D} - \frac{1}{\tanh(\beta \cdot D)} - \frac{1}{\tanh D} + \frac{1}{\sinh D}} \tag{30}$$

Moreover, the deflection $\eta(x)$ for each constituent beam according to Eqs. (9) and (10) can be expressed as follows

For the left span

$$\frac{\eta_L(x)}{f} = \frac{8 \cdot (\gamma_S - Z)}{Z + 1} \left[\frac{\cosh D(\beta/2 - x/L)}{D^2 \cdot \cosh(\beta \cdot D/2)} - \frac{1}{D^2} + \frac{1}{2} \cdot \frac{x}{L} \cdot \left(\beta - \frac{x}{L} \right) \right] + \frac{8 \cdot m}{Z + 1} \left[\frac{1}{\beta} \cdot \frac{x}{L} - \frac{\sinh(D \cdot x/L)}{\sinh(\beta \cdot D)} \right] \tag{31}$$

For the middle span

$$\begin{aligned} \frac{\eta(x)}{f} &= \frac{8 \cdot (\gamma - Z)}{(Z + 1)} \left[\frac{\cosh D(1/2 - x/L)}{D^2 \cdot \cosh(D/2)} - \frac{1}{D^2} + \frac{1}{2} \cdot \frac{x}{L} \cdot \left(1 - \frac{x}{L} \right) \right] \\ &+ \frac{8 \cdot m}{Z + 1} \left[1 - \frac{\sinh(D \cdot x/L) + \sinh(D - D \cdot x/L)}{\sinh D} \right] \end{aligned} \tag{32}$$

For the right span

$$\frac{\eta_R(x)}{f} = \frac{8 \cdot (\gamma_S - Z)}{Z + 1} \left[\frac{\cosh D(\beta/2 - x/L)}{D^2 \cdot \cosh(\beta \cdot D/2)} - \frac{1}{D^2} + \frac{1}{2} \cdot \frac{x}{L} \cdot \left(\beta - \frac{x}{L} \right) \right] + \frac{8 \cdot m}{Z + 1} \left[1 - \frac{1}{\beta} \cdot \frac{x}{L} - \frac{\sinh D(\beta - x/L)}{\sinh(\beta \cdot D)} \right] \tag{33}$$

According now to Eq. (15) the increase H_p of the cable force H_{g_0} , is related to the additional deflection η , through the following equation

$$\frac{H_p}{A_c E_{cc}} \cdot \sum L_c = \frac{g}{H_{g_0}} \int_0^{L_s} \eta_L dx + \frac{g}{H_{g_0}} \int_0^L \eta dx + \frac{g}{H_{g_0}} \int_0^{L_s} \eta_R dx \tag{34}$$

which, taking into account the introduced parameters, can be written

$$\frac{\varepsilon \cdot Z}{8 \cdot \lambda^2} \cdot s \cdot L = \int_0^{L_s} \eta_L dx + \int_0^L \eta dx + \int_0^{L_s} \eta_R dx \tag{35}$$

where

$$s = 2 \cdot \sqrt{\lambda^2 + \beta^2} [1 + (\lambda/\beta)^2 + 8 \cdot (\lambda \cdot \beta)^2] + (1 + 8 \cdot \lambda^2) \quad (36)$$

The unknown value Z may be determined from the condition that the deflection curve $\eta(x)$, according to Eqs. (31)-(33), must satisfy the “cable equation” (15). This equation is written in its final form as follows

$$\begin{aligned} \frac{\varepsilon \cdot Z \cdot (Z+1)}{(8 \cdot \lambda)^2} \cdot s = 2 \cdot (\gamma_S - Z) \cdot \left[\frac{2 \cdot \sinh(\beta \cdot D/2)}{D^3 \cdot \cosh(\beta \cdot D/2)} - \frac{\beta}{D^2} + \frac{\beta^3}{12} \right] \\ + (\gamma - Z) \cdot \left[\frac{2 \cdot \sinh(D/2)}{D^3 \cdot \cosh(D/2)} - \frac{1}{D^2} + \frac{1}{12} \right] + 2 \cdot m_{sym} \cdot \left[\frac{\beta+1}{2} - \frac{\cosh(\beta \cdot D) - 1}{D \cdot \sinh(\beta \cdot D)} - \frac{\cosh D - 1}{D \cdot \sinh D} \right] \end{aligned} \quad (37)$$

This transcendental equation is not directly solvable. Nevertheless it is possible to obtain quickly an accurate solution by the method of successive approximations, if as starting value Z_0 is taken that one which results from the previously examined model of the two-hinged main span girder, according to Eq. (24). It is important to note that the value of the solution Z of Eq. (37) is always less than Z_0 by no more than 8% and this fact allows its quick and accurate determination.

3. Determination of the maximum response

3.1 Two-hinged stiffening girder

In order to obtain the maximum values of the response, the following loading patterns have to be considered

1. For the maximum values of the cable force H_p , the live load p extends over the whole length of the girder.
2. For the maximum span bending moment M_{max} , as well the maximum deflection η_{max} , the live load p extends over the left (or the right) half of the central span.

The last two quantities, approximately located at the quarter of the span, can be directly determined according to the exact expression (9). Of course this procedure must be based on a value of Z which is determined for the specific location of the live load p , by taking into account the half value of it as previously stated.

Splitting the considered loading into a symmetric and an antisymmetric part as previously examined (Fig. 6), it is noted that the antisymmetric loading develops no additional cable force and the beam behaves like a simply supported one having the half span and subjected to the half live load. Then, superposing the relevant magnitudes at the quarter and at the middle of the span in the full and the half length beam respectively on the basis of Eq. (9) and taking into account the existing relation

$$M = -E \cdot I \frac{d^2 \eta}{dx^2} \quad (38)$$

the following expressions are obtained using the previously introduced dimensionless parameters.

$$\frac{M_{max}}{M_g^0} = -\frac{8 \cdot (\gamma - Z)}{D^2} \cdot \left[\frac{\cosh(D/4)}{\cosh(D/2)} - 1 \right] - \frac{8 \cdot \gamma}{D^2} \cdot \left[\frac{1}{\cosh(D/4)} - 1 \right] \quad (39)$$

and

$$\frac{\eta_{max}}{L} = \frac{8 \cdot \lambda \cdot (\gamma - Z)}{(Z + 1) \cdot D^2} \cdot \left[\frac{\cosh(D/4)}{\cosh(D/2)} + \frac{3 \cdot D^2}{32} - 1 \right] + \frac{8 \cdot \lambda \cdot \gamma}{(Z + 1) \cdot D^2} \cdot \left[\frac{1}{\cosh(D/4)} + \frac{D^2}{32} - 1 \right] \quad (40)$$

where

$$M_g^0 = \frac{g \cdot L^2}{8} \quad (41)$$

represents the bending moment of the freely supported beam of length L under the dead load g .

3.2 Continuous stiffening girder

In order to obtain the maximum values of the response, the following loading patterns have to be considered (Fig. 8)

1. For the maximum values of the cable force H_p , the live load p extends over the whole length of the bridge.
2. For the maximum span bending moment M_{max} , as well the maximum deflection η_{max} , the live load p extends over the left half of the central span.
3. For the support moments $minM_s$ and $maxM_s$, yielding the maximum tensile stress at the top and

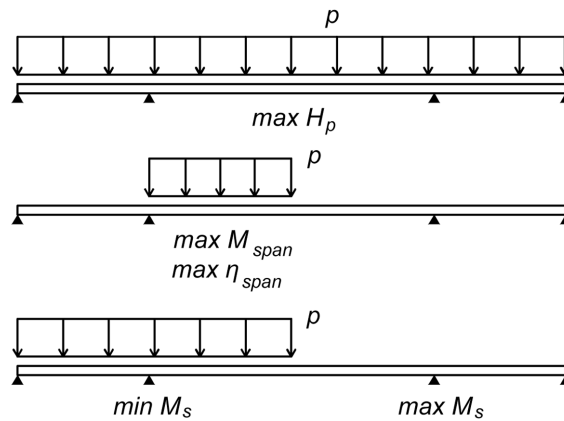


Fig. 8 Characteristic positions of live load for maximum response

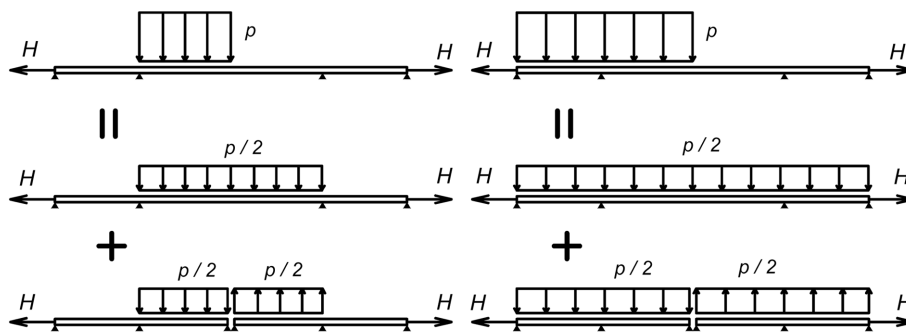


Fig. 9 Splitting of loading in symmetrical and antisymmetrical part

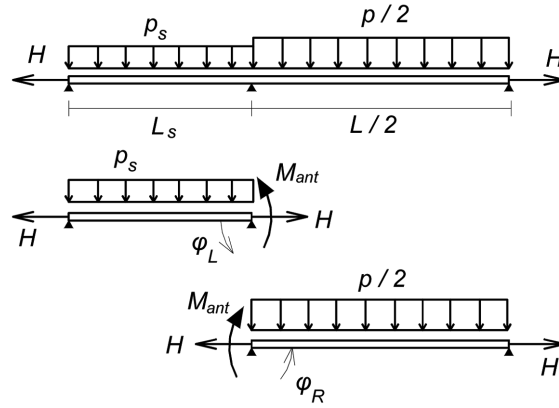


Fig. 10 Fictitious beam for antisymmetrical loading

bottom fibers of the girder respectively, the live load p extends from the left end of the bridge to the center of the main span.

In the above second and third cases the loading is considered as superposition of a symmetrical ($p/2$) and an antisymmetrical ($p/2$) one (Fig. 9). As the antisymmetrical loading ($p/2$) does not yield a cable force according to Eq. (16), the cable force results each time from the symmetrical loading ($p/2$) only. However, the antisymmetrical loading ($p/2$) applies to the modified continuous beam as shown in Fig. 10 and, as the loading term (H_p/R) vanishes, it provides an essential contribution to the final values of bending moments as well as the girder deflections. It is noted that the above superposition is valid, as the tension load ($H_g + H_p$) is held constant.

Considering now the fictitious modified continuous beam as shown in Fig. 10, the support moment M_{ant} is determined by requiring the end slopes ϕ_L and ϕ_R of the constituent simple beams at the inner support to be equal. The following expression is obtained

$$M_{ant} = g \cdot L^2 \cdot m_{ant} \tag{42}$$

where

$$m_{ant} = \frac{1}{D^2} \frac{(\gamma_s) \cdot [(\beta \cdot D/2) - \tanh(\beta \cdot D/2)] + (\gamma/2) \cdot [D/4 - \tanh(D/4)]}{\frac{2}{D} + \frac{1}{\beta \cdot D} - \frac{1}{\tanh(\beta \cdot D)} - \frac{1}{\tanh(D/2)}} \tag{43}$$

Examining first the above *Case 2*, M_{max} and η_{max} which are approximately located at the quarter point of the central span, are determined by superposing their value due to the symmetrical loading ($p/2$) on the complete system with that one at the center of the right span of the above modified continuous beam, under the loading ($p/2$). It is

$$M_{max} = -EI \cdot \left(\frac{d^2 \eta_{sym}}{dx^2} \right)_{(x=L/4)} - EI \cdot \left(\frac{d^2 \eta_{ant}}{dx^2} \right)_{(x=L/4)} \tag{45}$$

and

$$\eta_{max} = (\eta_{sym})_{(x=L/4)} + (\eta_{ant})_{(x=L/4)} \tag{46}$$

where η_{sym} is the deflection function of the central span under the symmetrical load ($p/2$) and η_{ant} is the deflection function of the right span ($L/2$) of the modified continuous beam under the same load, according to Fig. 10.

On the basis of Eqs. (9), (10) and Eqs. (44), (45), as well as of previous considerations, it is obtained

$$\frac{M_{max}}{g \cdot L^2} = \frac{(\gamma/2 - Z)}{D^2} \left[\frac{\cosh(D/4)}{\cosh(D/2)} - 1 \right] + m_{sym} \left[1 - \frac{\sinh(D/4) + \sinh(3 \cdot D/4)}{\sinh D} \right] - \frac{(\gamma/2)}{D^2} \left[\frac{1}{\cosh(D/2)} - 1 \right] + m_{ant} \frac{\sinh(D/4)}{\sinh(D/2)} \quad (47)$$

and

$$\frac{\eta_{max}}{L} = \frac{8 \cdot \lambda \cdot (\gamma/2 - Z)}{Z + 1} \left[\frac{\cosh(D/4)}{D^2 \cdot \cosh(D/2)} - \frac{1}{D^2} + \frac{3}{32} \right] + \frac{8 \cdot \lambda}{Z + 1} \cdot m_{sym} \cdot \left[1 - \frac{\sinh(D/4) + \sinh(3 \cdot D/4)}{\sinh D} \right] + \frac{8 \cdot \lambda \cdot (\gamma/2)}{Z + 1} \left[\frac{1}{D^2 \cdot \cosh(D/4)} - \frac{1}{D^2} + \frac{1}{32} \right] + \frac{8 \cdot \lambda}{Z + 1} \cdot m_{ant} \cdot \left[\frac{1}{2} - \frac{\sinh(D/4)}{\sinh(D/2)} \right] \quad (48)$$

where m_{sym} and m_{ant} are taken from Eqs. (30) and (43) respectively.

The examination of *Case 3* as previously explained, gives the following results, on the basis of Eqs. (29) and (42)

$$\frac{\min M_s}{g \cdot L^2}, \frac{\max M_s}{g \cdot L^2} = \frac{1}{D^2} \frac{(\gamma/2 - Z) [\beta \cdot D/2 - \tanh(\beta \cdot D/2) + D/2 - \tanh(D/2)]}{\beta \cdot D - \frac{1}{\tanh(\beta \cdot D)} - \frac{1}{\tanh D} + \frac{1}{\sinh D}} \pm \frac{1}{D^2} \frac{(\gamma/2) [\beta \cdot D/2 - \tanh(\beta \cdot D/2) + D/4 - \tanh(D/4)]}{\frac{2}{D} + \frac{1}{\beta \cdot D} - \frac{1}{\tanh(\beta \cdot D)} + \frac{1}{\tanh(D/2)}} \quad (49)$$

where the alternative plus and minus sign in the equations, refers to the $\min M_s$ and $\max M_s$ respectively.

As already noticed for the last two cases, in the expressions 46 ÷ 48 that value of Z is considered, which is obtained from the symmetrical loading ($p/2$) on the system.

4. Numerical procedure

Once the design data of a suspension bridge are known, namely the main and side span lengths L and L_s respectively, the cable sags f (approximately equal to the tower height) and f_s (according to Eq. (2)), the cable section A_c , the permanent load g , the live load p , the girder moment of inertia I and the moduli of elasticity E and E_c for the girder and cable respectively, the procedure of the analysis goes along the following steps, which can be directly performed by a computer program

4.1 Two-hinged stiffening girder

1. Determination of the four dimensionless parameters G , λ , γ , and ε through Eqs. (3) and (22), on the basis of H_g calculated from Eq. (1)
2. Determination of the value Z and consequently of H_p from Eq. (25), according to the expressions (24) and (26), as well as of the bending moment M_g^0 of the simply supported girder through Eq. (41).

3. Determination of the ratio Z from Eq. (25) anew, by taking into account the half value of the parameter γ previously used.
4. Evaluation of the magnitudes M_{max} and η_{max} from the Eqs. (39) and (40) respectively, after determination of the respective value D from Eq. (28)

4.2 Continuous stiffening girder

1. Determination of the five dimensionless parameters G , λ , β , γ , and ε through Eqs. (3) and (21), on the basis of H_g calculated from Eq. (1)
2. Determination of the value Z_0 through Eq. (25), according to the expressions (24) and (26).
3. Determination of the maximum cable force from Eq. (37) using the expression (30), through successive approximations, substituting for $\gamma_s = \gamma$ in both equations and using Z_0 as the starting value. The procedure converges rapidly to a smaller value differing not more than 8% from the initial one.
4. Evaluation of M_{max} and η_{max} from Eqs. (47) and (48) respectively, after determination of the value Z from Eq. (30) using expression (37), by substituting for “ γ_s ” and “ γ ”, the values 0 and $\gamma/2$ respectively
5. Evaluation of $minM_s$ and $maxM_s$ from Eq. (49), after determination of the value Z from Eq.(37) using expression (30), by substituting for both “ γ_s ” and “ γ ”, the value $\gamma/2$.

5. Parametric study

On the basis of the above relations and for the constant values of $\lambda = 0.1$ and $\varepsilon = 0.002$ which represent logical design decisions, the diagrams showing the variation of the ratios (H_p/H_g) , (M_{max}/M_g^0) and (η_{max}/L) are first determined (Figs. 11 to 16), for the cases of hinged and continuous girder having a span ratio β equal to 0.35. The influence of the variation of β in the case of continuous girder is also separately considered under a constant value of $\gamma = 0.20$ and depicted in Figs. 19 to 21

The ratio (H_p/H_g) is, for both the cases of hinged and continuous girder, independant of the stiffness factor G , depending only on the loading ratio γ (Figs. 11 and 12, respectively). This ratio

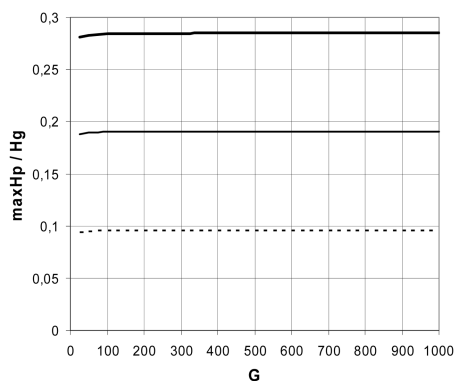


Fig. 11 Maximum cable force H_p for hinged girder

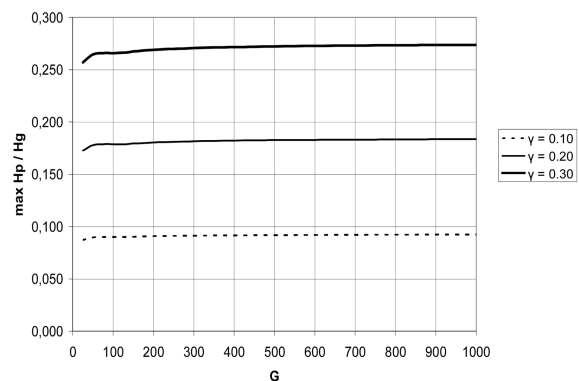


Fig. 12 Maximum cable force H_p for continuous girder ($\beta = 0.35$)

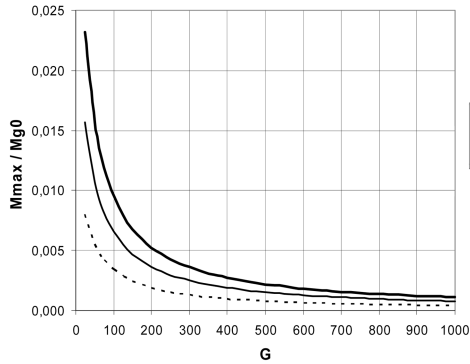


Fig. 13 Maximum span bending moment for hinged girder

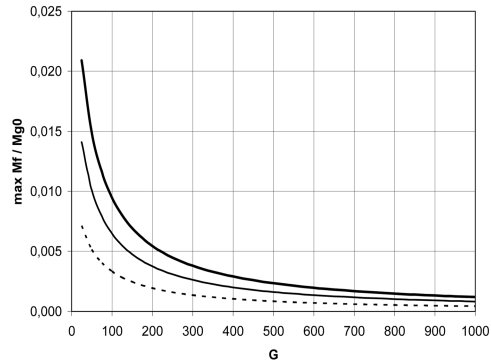


Fig. 14 Maximum span bending moment for continuous girder ($\beta = 0.35$)

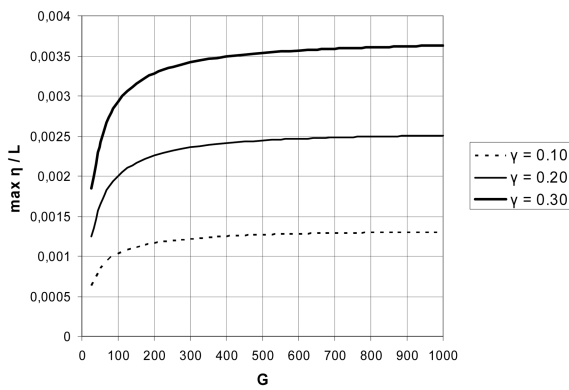


Fig. 15 Maximum deflection for hinged girder

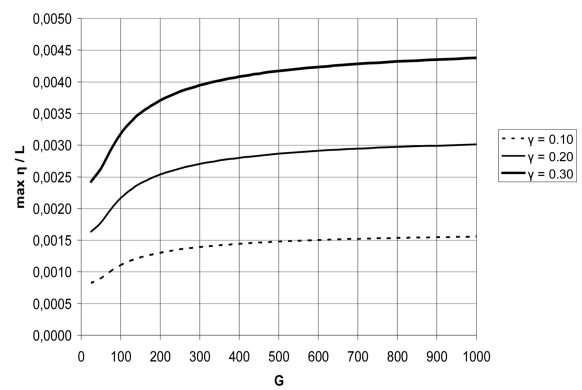


Fig. 16 Maximum deflection for continuous girder ($\beta = 0.35$)

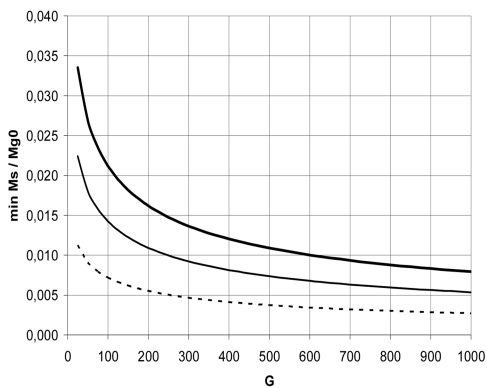


Fig. 17 Maximum support bending moment causing upper fiber tension ($\beta = 0.35$)

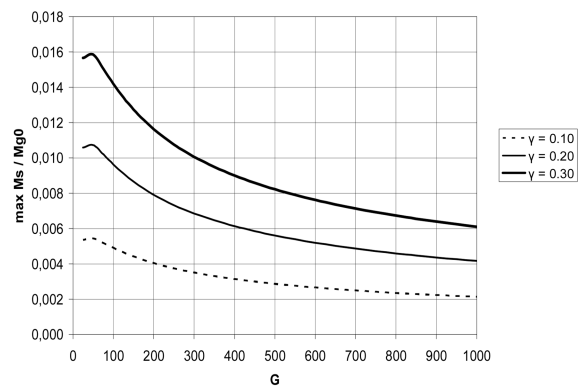


Fig. 18 Maximum support bending moment causing lower fiber tension ($\beta = 0.35$)

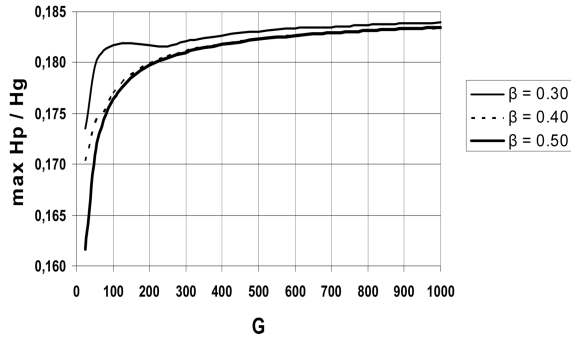


Fig. 19 Influence of β on the maximum cable force H_p ($\gamma = 0.20$)

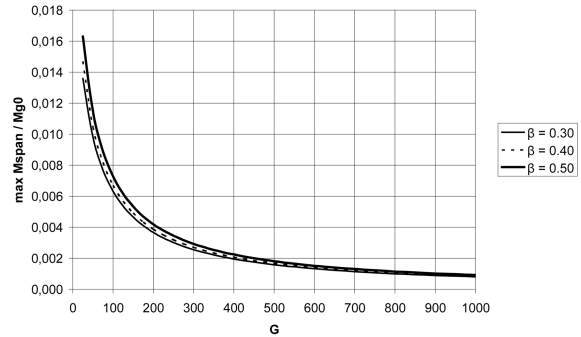


Fig. 20 Influence of β on the maximum span bending moment ($\gamma = 0.20$)

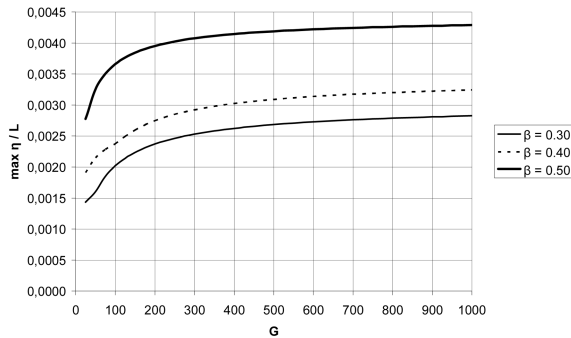


Fig. 21 Influence of β on the maximum deflection ($\gamma = 0.20$)

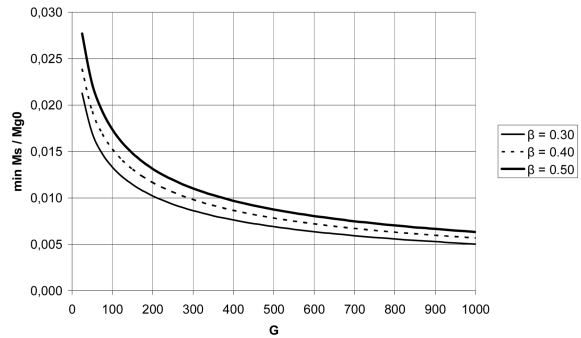


Fig. 22 Influence of β on minimum support bending moment ($\gamma = 0.20$)

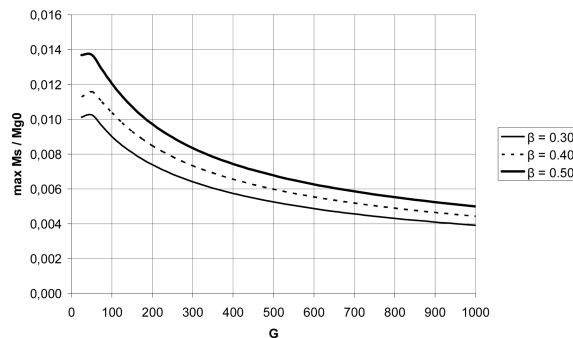


Fig. 23 Influence of β on maximum support bending moment ($\gamma = 0.20$)

results slightly less than γ , whereas the variation of the span ratio β , in the case of continuous girder, does not affect its value practically at all for values of G greater than 200 (Fig. 19). The values of the ratio are slightly less in the case of continuous girder than in the hinged one. The above results are in good agreement with those found by (Chen *et al.* 2006), regarding the estimation of the cable safety factor.

The ratio (M_{max}/M_g^0) is, for both cases of hinged and continuous girder, very little influenced from the parameter γ , as long the values of G are greater than 450 (Figs. 13 and 14, respectively), whereas it is absolutely unaffected from the variation of β (Fig. 20). The values of this ratio are slightly greater in the continuous girder than in the hinged one.

The ratio (η_{max}/L) is, for both cases of hinged and continuous girder, practically unaffected by values of G greater than 300 (Figs. 15 and 16, respectively). However, increasing the span ratio β , leads to an increase of this value (Fig. 21). The values of this ratio are somewhat greater in the continuous girder than in the hinged one. From the Figs. 15 and 16 it may be readily certified that for very long spans, the stiffening contribution of the girder becomes negligible – an already known conclusion (e.g., Cobo *et al.* 2001 and Clemente *et al.* 2000) -, while for moderate spans this contribution is clear as may be seen from the left portion of the curves. Moreover from the same diagrams it may be concluded that increasing the dead load leads to an increase of the structure's stiffness, as already mentioned in (Imai and Frangopol 2000 and Cobo *et al.* 2001).

The support bending moment $minM_s$ causing the maximum tension on the upper fibers of the girder, governs the design of the stiffening girder, as its value is about three times more than M_{max} for a given stiffness factor G (Fig. 17). It is also very little affected from the span ratio β (Fig. 22).

The support bending moment $maxM_s$ causing tension on the lower fibers of the girder - a peculiarity in itself regarding the nature of the continuous beam - is less than the respective $minM_s$ for a given stiffness factor G , but it is more than the double of the maximum span moment M_{max} (Fig. 18). An increase of the span ratio β leads to an increase of the ratio $(maxM_s/M_g^0)$, for a given loading ratio γ (Fig. 23).

6. Conclusions

The problem of evaluating the static response of a suspension bridge with hinged or continuous stiffening girder, under the additional action of the live load can be tackled directly with a minimum computing effort. It is shown that the response is totally determined on the basis of five dimensionless parameters, namely the sag-to-span of the cable (λ), the initial strain of the cable at its lowest point under the dead load (ε), the loading ratio (γ), the stiffness factor (G) and the side-span ratio (β). The procedure followed permits also the establishment of diagrams which show the influence of the above design parameters on the response and moreover they allow very quickly its quantitative assessment. However it should be pointed out that selecting a continuous stiffening girder for long spans, does not improve the static performance as compared to the hinged-type alternative, because of the high support moments, whereas the resulting span moments and deflections are not decreased as could be expected. As it has been mentioned earlier, the continuity of the girder concerns rather a constructional decision than the improvement of the structural performance.

References

- Arzoumanidis, S.G. and Bienek, M.P. (1985), "Finite element analysis of suspension bridges", *Comput. Struct.*, **21**(6), 1237-1256.
- Brotton, D.M. and Arnold, G. (1963), "The solution of suspension bridge problems by digital computers", *Struct.*

- Eng.*, **41**(7), 213-222.
- Cheng, J. and Xiao, R.C. (2006), "Application of inverse reliability method to estimation of cable safety factors of long span suspension bridges", *Struct. Eng. Mech.*, **23**(2), 195-207.
- Clemente, P., Nicolosi, G. and Raithel, A. (2000), "Preliminary design of very long-span suspension bridges", *Eng. Struct.*, **22**(12), 1699-1706.
- Cobo del Arco, D. and Aparicio, A.C. (2001), "Preliminary static analysis of suspension bridges", *Eng. Struct.*, **23**(9), 1096-1103.
- Imai, K. and Frangopol, D. (2000), "Response prediction of geometrically nonlinear structures", *J. Struct. Eng.*, ASCE, **126**(11), 1348-1355.
- Jennings, A. and Mairs, J.E. (1972), "Static analysis of suspension bridges", *J. Struct. Div.*, ASCE, **98**(11), 2433-2455.
- Liu, C., Wang, T.L. and Qin, Q. (1999), "Study on sensitivity of modal parameters for suspension bridges", *Struct. Eng. Mech.*, **8**(5), 453-464.
- O'Connor, C. (1971), *Design of Bridge Superstructures*, Wiley, New York.
- Roik, K. (1983), *Steel Structures* (in German), Wilhelm Ernst & Sohn, Berlin.
- Ryall, M.J., Parke, G.A.R. and Harding, J.E. (2000), *Manual of Bridge Engineering*, Thomas Telford Publishing, London.
- Steinman, D.B. (1935), "A generalized deflection theory for suspension bridges", *Trans. ASCE*, **100**, 1133-1170.
- Timoshenko, S. (1943), "Theory of suspension Bridges", *J. Franklin Inst.*, **235**(3), 231-238; **235**(4), 327-349.
- Timoshenko, S. (1956), *Strength of Materials Part II*, D. Van Nostrand Company Inc., New York.
- W.F. Chen and Lian, Duan (1999), *Bridge Engineering*, CRC Press, Florida U.S.A.
- Wollmann, G.P. (2001), "Preliminary analysis of suspension bridges", *J. Bridge Eng.*, ASCE, **6**(4), 227-233.